Title

Development of a scalable method to isolate subsets of stem cell-derived pancreatic islet cells

Journal

Stem Cell Reports, 17(4)

ISSN

2213-6711

Authors

Parent, Audrey V
Ashe, Sudipta
Nair, Gopika G
et al.

Publication Date

2022-04-01

DOI

10.1016/j.stemcr.2022.02.001

Peer reviewed

Stem Cell Reports
Resource
ISSCR
OPEN ACCESS

Development of a scalable method to isolate subsets of stem cell-derived pancreatic islet cells

Audrey V. Parent,[1,*] Sudipta Ashe,[1] Gopika G. Nair,[1] Mei-Lan Li,[1] Jessica Chavez,[1] Jennifer S. Liu,[1] Yongping Zhong,[2] Philip R. Streeter,[2] and Matthias Hebrok[1,*]
[1]Diabetes Center, Department of Medicine, University of California, San Francisco, San Francisco, CA 94143, USA
[2]Oregon Stem Cell Center, Oregon Health and Science University, Portland, OR 97239, USA
*Correspondence: audrey.parent@ucsf.edu (A.V.P.), matthias.hebrok@ucsf.edu (M.H.)
https://doi.org/10.1016/j.stemcr.2022.02.001

SUMMARY

Cell replacement therapy using β cells derived from stem cells is a promising alternative to conventional diabetes treatment options. Although current differentiation methods produce glucose-responsive β cells, they can also yield populations of undesired endocrine progenitors and other proliferating cell types that might interfere with long-term islet function and safety of transplanted cells. Here, we describe the generation of an array of monoclonal antibodies against cell surface markers that selectively label stem cell-derived islet cells. A high-throughput screen identified promising candidates, including three clones that mark a high proportion of endocrine cells in differentiated cultures. A scalable magnetic sorting method was developed to enrich for human pluripotent stem cell (hPSC)-derived islet cells using these three antibodies, leading to the formation of islet-like clusters with improved glucose-stimulated insulin secretion and reduced growth upon transplantation. This strategy should facilitate large-scale production of functional islet clusters from stem cells for disease modeling and cell replacement therapy.

INTRODUCTION

Pancreatic β cells regulate metabolic homeostasis by synthesizing, storing, and releasing insulin to maintain circulating glucose concentrations within physiological range. Destruction (type I) or dysfunction (type II) of β cells causes an elevation in blood glucose levels, leading to the development of diabetes. In addition to traditional therapeutic interventions that include frequent insulin administration, transplantation of functional pancreatic islets from cadaveric donors has emerged as an efficient treatment option to restore blood glucose to physiological levels. However, limited islet supply remains a critical barrier preventing the broad application of this promising therapy (Sneddon et al., 2018). An alternative source of β cells for such transplantations would be islets cells derived from *in vitro* differentiation of human pluripotent stem cells (hPSCs) (Nair et al., 2020). Several multistage strategies leading to the production of functional human β cells from hPSCs *in vitro* have been reported (Nair et al., 2019b; Pagliuca et al., 2014; Rezania et al., 2014; Russ et al., 2015; Velazco-Cruz et al., 2019). Although these protocols generate functional insulin-producing cells, the differentiated cultures can also contain additional populations of cells, such as multihormonal cells, endocrine progenitors, or other undesirable proliferating cell types that may interfere with islet function or graft safety. Notably, the maturation and safety of hPSC-derived β cell differentiations can be further increased by recapitulating endocrine cell clustering to form enriched β clusters (eBCs) (Nair et al., 2019b). This method enables the generation of mature β cells by sorting based on the expression of insulin at the immature β-like stage. The purification method reported in this study, however, requires cell sorting of a transgenic hPSC line in which a Green Fluorescent Protein (GFP) reporter gene has been inserted into the endogenous human insulin locus, which limits its use for cell therapy. We thus aimed to replicate the same strategy but using cell surface markers expressed on immature cells instead of relying on a reporter cell line.

Although surface markers may serve as an alternative to purify relevant cell populations during *in vitro* β cell differentiation, identifying antibodies capable of specifically isolating large numbers of hPSC-derived β cells remains challenging. Antibody-mediated cell sorting has been used to isolate anterior definitive endoderm (Mahaddalkar et al., 2020) or pancreatic progenitors that can differentiate into β cells (Ameri et al., 2017; Cogger et al., 2017; Kelly et al., 2011). The clusters generated with these approaches had a higher proportion of β cells than unsorted clusters, but the resulting percentage of insulin-expressing cells at the β-like stage still remained below 50%. A method to enrich for β cells using a cell surface antibody against CD49a was also reported (Veres et al., 2019). Although the typical yield of cells recovered after purification with this antibody was low (<10% of cells), the sorting enhanced functional maturation of hPSC-derived β cells, suggesting that antibody-based magnetic sorting of β-like cells could provide the same benefits as GFP-based fluorescence-activated cell sorting (FACS) but with greater scalability.

Here, we generated more than a thousand monoclonal antibodies (mAbs) against cell surface markers that

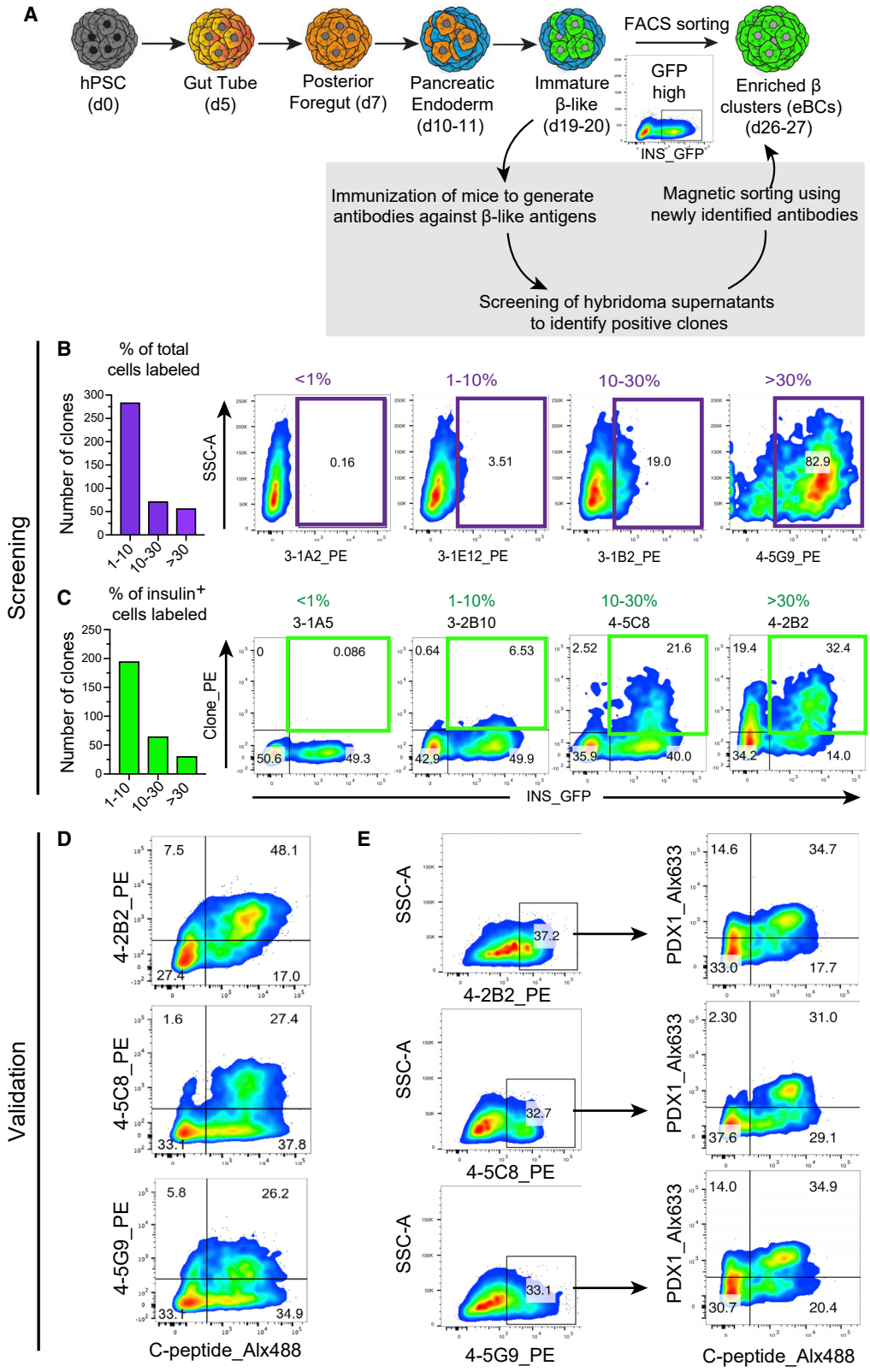

(legend on next page)

selectively label stem cell-derived endocrine cell subsets. A high-throughput screening assay was employed to identify promising antibodies, including three clones that mark a high fraction of β cell progenitors derived from hPSCs. A scalable magnetic sorting method was developed to enrich for hPSC-derived β-like cells using these antibodies, leading to the formation of islet-like clusters with increased maturation and safety. These antibodies thus selectively isolate islet cell populations from hPSCs differentiated *in vitro* using a scalable magnetic sorting approach, facilitating the large-scale production of functional islet-like clusters from stem cell cultures.

RESULTS

Generation of mAbs recognizing cell surface antigens of hPSC-derived pancreatic cells

Previous studies have shown that the insulin secretory profile of hPSC-derived β cells can be improved by enriching for immature β-like cells followed by reaggregation of the cells (Nair et al., 2019b; Veres et al., 2019). However, these methods either require the use of cell sorters, which limits the total numbers of cells that can be processed at once, or had low recovery of insulin-expressing cells. In addition, although the generation of antibodies directed against pancreatic antigens has enabled isolation of mature, adult β cells from primary islets (Dorrell et al., 2008, 2016), these antibodies do not efficiently enrich for C-peptide$^+$ cells from immature stem cell-derived β-like cells (Figures S1A and S1B). To develop alternative endocrine clustering strategies that are more efficient and scalable, we thus set out to generate new antibodies against cell surface markers present in hPSC-derived immature islet cell populations generated using our published protocol (Nair et al., 2019b). We employed a subtractive immunization strategy to generate mouse anti-human mAbs against surface proteins present on day (d) 19–20 insulin-expressing cells derived from insulin (INS)-GFP human embryonic stem cells (hESCs) (Figures 1A and S1C). These insulin-expressing cells include immature β, α, and δ cells (Nair et al., 2019b; Russell et al., 2020). This approach led to the production of 1,248 hybridoma clones that were screened by high-throughput flow cytometry for their specificity to cell surface epitopes present on d19–20 insulin-expressing cells. The gating strategy for the screen is shown in Figure S1D. We first excluded clones that labeled <1% of the cells at d19–20. From the 413 remaining clones, we identified approximately 68% that labeled between 1% and 10% of all cells (284/413), 17% that labeled between 10% and 30% (72/413), and 14% that labeled >30% (57/413) (Figure 1B). Representative examples of each category of clones are shown in Figure 1B. Next, we categorized the clones based on the percentage of insulin-expressing GFP$^+$ cells that were labeled by the mAbs. Approximately 67% of the clones showing positivity for insulin-expressing cells labeled <10% of the cells (195/291), while 22% labeled 10%–30% (65/291) and 11% labeled >30% (31/291) (Figure 1C). Representative examples of each category of clones are shown in Figure 1C.

From this screen, we selected three clones that had high specificity for insulin-expressing cells (clones 4-2B2, 4-5C8, and 4-5G9) and confirmed that the staining pattern was retained after expansion of the hybridoma cells (Figures S1E and S1F). Flow cytometric analysis using secondary antibodies specific for either mouse IgG or IgM isotypes indicated that all three clones were IgM isotypes (Figure S1G). These three mAbs, which reproducibly labeled a significant fraction of GFP$^+$ cells in the culture, were further assessed for co-expression with C-peptide and PDX1. Cells differentiated up to d19–20 were first stained with hybridoma supernatants followed by permeabilization and intracellular staining for C-peptide and PDX1 antibodies prior to quantification by flow cytometry. As shown in Figure 1D, all three mAbs stained a subset of C-peptide$^+$ cells, with 4-2B2 labeling most of the C-peptide$^+$ cells present in the differentiated cultures. In addition, many of the cells that were labeled with each mAb were also positive for PDX1, a β cell marker (Figure 1E). These data thus confirm that our screen identified three promising mAbs that mark insulin-expressing cells derived from hPSCs.

4-2B2-mediated cell sorting generates clusters enriched for β cells

To evaluate the potential of the newly identified antibodies to serve as an alternative to GFP sorting, we used the 4-2B2 clone for FACS of immature β-like cells (Figure 2A). We selected this mAb based on the high percentage of co-labeling with C-peptide$^+$ cells (Figure 1D). Sorted cells were reaggregated into eBCs in pre-patterned chambers of

Figure 1. Generation of monoclonal antibodies recognizing cell surface antigens of hPSC-derived pancreatic cells

(A) Schematic outlining the differentiation protocol to generate pancreatic β-like cells from hPSCs and sorting methods to form enriched β clusters (eBCs). More details on the culture conditions are included in the *Experimental Procedures* section. (B) Quantification of the number of clones that bound 1%–10%, 10%–30%, or >30% of all cells. Representative examples of each category of clones are shown. (C) Quantification of the number of clones that bound 1%–10%, 10%–30%, or >30% insulin-expressing cells. Representative examples of each category of clones are shown. (D) Flow cytometric analysis of the percentage of cells co-stained for C-peptide and clones 4-2B2, 4-5C8, or 4-5G9. (E) Flow cytometric analysis of PDX1 and C-peptide expression in 4-2B2$^+$, 4-5C8$^+$, and 4-5G9$^+$ cells. See also Figure S1.

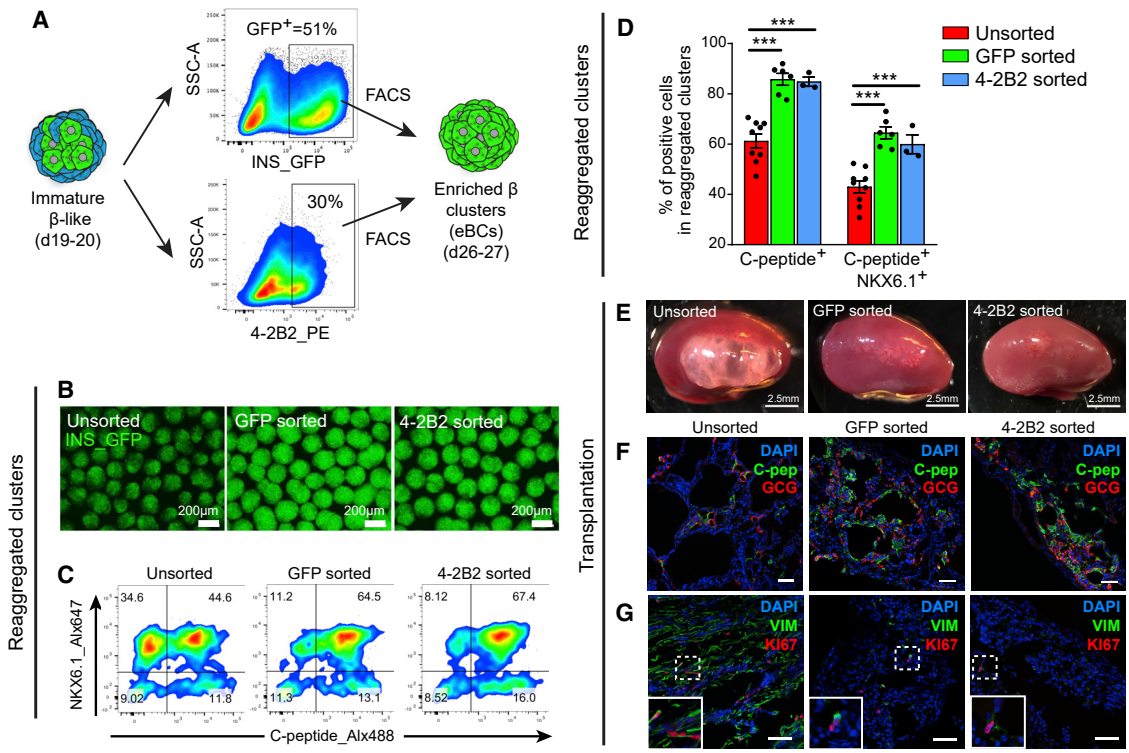

Figure 2. 4-2B2-mediated cell sorting generates clusters enriched for β cells

(A) Schematic of gating strategy used for FACS based on GFP expression or 4-2B2 labeling.

(B) Fluorescence images of unsorted, GFP sorted, and 4-2B2 sorted eBCs after transfer in suspension plates. Scale bars, 200 μm. (C and D) Representative FACS plots (C) and quantification (D) of C-peptide$^+$ and NKX6.1$^+$ cells in unsorted, GFP sorted, and 4-2B2 sorted eBCs. Data are represented as mean ± SD. Each point is an independent experiment. ***$p < 0.001$ determined by two-tailed unpaired t test. (E) Images of kidneys from mice transplanted with unsorted, GFP sorted, or 4-2B2 sorted clusters. Kidneys were harvested 12 weeks post-transplantation. n = 2 for GFP and n = 3 for unsorted and 4-2B2 sorted grafts. The occurrence of overgrown structures was 3/3 for unsorted, 1 very small structure in 1/2 GFP grafts, and 0/3 for 4-2B2 grafts. (F) Immunofluorescence images of unsorted, GFP sorted, or 4-2B2 sorted grafts stained with DAPI (blue), C-peptide (C-pep, green), and glucagon (GCG, red). Scale bars, 50 μm. (G) Immunofluorescence images of unsorted, GFP sorted, or 4-2B2 sorted grafts stained with DAPI (blue), vimentin (green), and Ki67 (red). Scale bars, 50 μm.

AggreWell-400 plates at a density of ~1,000 cells per cluster to simulate the average number of β cells in one human islet equivalent (Pisania et al., 2010). GFP sorted and unsorted cells served as positive and negative controls, respectively. GFP$^+$ and 4-2B2$^+$ sorted cells formed similar-sized clusters (~100–200 μm) with increased GFP intensity when compared with unsorted cells (Figure 2B). Characterization of the eBCs by flow cytometry revealed similar levels of enrichment of C-peptide$^+$ in both GFP$^+$ and 4-2B2$^+$ sorted eBCs (85.8% ± 5.8% and 84.8% ± 3.2%) compared with unsorted clusters (61.2% ± 8.3%), as well as increased proportion of C-peptide$^+$/NKX6.1$^+$ β cells (64.5% ± 5.8% in GFP sorted eBCs, 60.0% ± 6.5% in 4-2B2 eBCs, and 43.0% ± 7.2% in unsorted clusters) (Figures 2C and 2D).

To test the growth potential of 4-2B2 FACS-sorted eBCs *in vivo*, we transplanted unsorted clusters, as well as GFP and 4-2B2 sorted eBCs, under the kidney capsule of non-diabetic NOD.Cg-Prkdc^{scid} Il2rg^{tm1Wjl}/SzJ (NSG) mice. As shown in Figure 2E, grafts of GFP and 4-2B2 sorted eBCs appeared similar in size 12 weeks after transplantation, while grafts of unsorted cells had expanded to form extraneous structures, indicative of the presence of contaminating cells with high proliferative capacity. Immunofluorescence analysis of harvested grafts confirmed that both GFP and 4-2B2 grafts were enriched for C-peptide$^+$ and glucagon$^+$ cells over unsorted grafts (Figure 2F), while proliferating vimentin$^+$ cells were reduced (Figure 2G). These experiments thus demonstrate that, similar to what is observed with GFP purification, sorting using the 4-2B2 mAb enriches for endocrine cells while removing cells that overly proliferate *in vivo*.

Generation of functional eBCs via scalable magnetic sorting

To develop a purification method that is more scalable than FACS, we stained immature β-like cells with the most promising antibodies (4-2B2, 4-5C8, and 4-5G9) and used

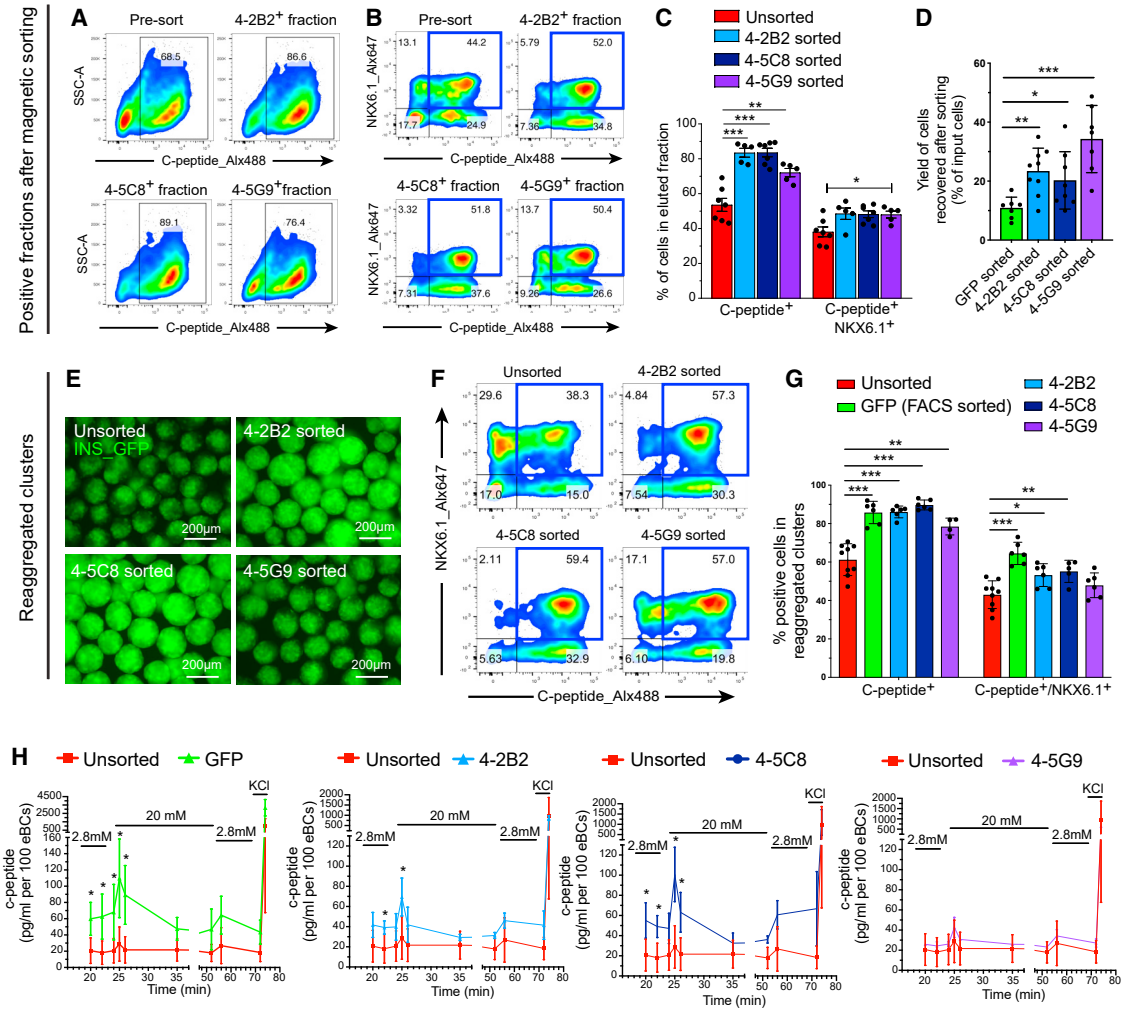

Figure 3. Generation of functional eBCs via scalable magnetic sorting

(A–C) Representative FACS plots and quantification of C-peptide$^+$ (A and C) and C-peptide$^+$/NKX6.1$^+$ (B and C) cells in pre-sorted samples or eluted fractions following magnetic sorting with the 4-2B2, 4-5C8, and 4-5G9 mAbs. Data are represented as mean ± SD. Each point is an independent experiment. *$p < 0.05$, **$p < 0.01$, and ***$p < 0.001$ determined by two-tailed unpaired t test. (D) Quantification of the percentage of input cells recovered after GFP-based FACS or magnetic bead sorting using the 4-2B2, 4-5C8, or 4-5G9 clones. *$p < 0.05$, **$p < 0.01$, and ***$p < 0.001$ determined by two-tailed unpaired t test. (E) Fluorescence images of unsorted, 4-2B2 sorted, 4-5C8 sorted, and 4-5G9 sorted eBCs 1 week after magnetic enrichment. Scale bars, 200 μm. (F and G) Representative FACS plots (F) and quantification (G) of C-peptide$^+$ and NKX6.1$^+$ cells in unsorted, GFP FACS sorted, 4-2B2 MACS sorted, 4-5C8 MACS sorted, and 4-5G9 MACS sorted eBCs 1 week after enrichment. Data are represented as mean ± SD. Each point is an independent experiment. *$p < 0.05$, **$p < 0.01$, and ***$p < 0.001$ determined by two-tailed unpaired t test. (H) Dynamic secretion of C-peptide in response to stimulation with 20 mM glucose and 30 mM KCl in an *in vitro* perifusion assay. The starting basal glucose concentration was 2.8 mM. n = 3–4 independent experiments. Data are represented as mean ± SD. *$p < 0.05$ determined by two-tailed unpaired t test. See also Figure S2.

magnetic beads to enrich for labeled cells. Analysis of positively selected cells showed that sorting with each clone enriched for C-peptide$^+$ cells over pre-sorted samples (53.6% ± 9.8% in pre-sorted, 83.5% ± 5.7% in 4-2B2$^+$, 83.6% ± 6.7% in 4-5C8$^+$, and 72.1% ± 5.3% in 4-5G9$^+$ fractions) (Figures 3A and 3C). Similar results were obtained for C-peptide$^+$/NKX6.1$^+$ β cells (38.1% ± 7.4% in pre-sorted, 48.5% ± 7.3% in 4-2B2$^+$, 48.2% ± 5.1% in 4-5C8$^+$, and 48.0% ± 4.4% in 4-5G9$^+$ fractions) (Figures 3B and 3C). Notably, the average number of cells recovered when starting with 1 × 10^6 cells was about 2.3 × 10^5 cells (23% of input cells), 2 × 10^5 (20% of input cells), or 3.4 × 10^5 (34% of input cells) for the 4-2B2 clone, the 4-5C8 clone, and the 4-5G9 clone, respectively, an increase over the 1.2 × 10^5 cells (12% of input cells) typically obtained when sorting GFP$^+$ cells (Figure 3D).

Magnetically separated cells seeded in pre-patterned micro-wells reorganized into clusters of comparable size (~100–200 μm), with 4-2B2 and 4-5C8 sorted clusters having the highest GFP intensity (Figure 3E). In addition to the pre-patterned plates, a reaggregation method using suspension plates was tested, resulting in clusters with similar morphology but slightly bigger size (~150–250 μm) (Figure S2A). Quantitative assessment via flow cytometry revealed significant enrichment of C-peptide$^+$ cells relative to unsorted clusters with all three mAbs (61.2% ± 8.3% in unsorted clusters, 86.1% ± 3.1% in 4-2B2 eBCs, 89.7% ± 2.6% in 4-5C8 eBCs, and 78.5% ± 4.4% in 4-5G9 eBCs), while C-peptide$^+$/NKX6.1$^+$ cells were significantly enriched with the 4-2B2 and 4-5C8 clones (43.0% ± 7.2% in unsorted clusters, 53.2% ± 5.9% in 4-2B2 eBCs, 55.1% ± 5.8% in 4-5C8 eBCs, and 48.9% ± 7.2% in 4-5G9 eBCs) (Figures 3F and 3G). Gene expression analysis by qPCR confirmed an increase in insulin (*INS*) and *PDX1* expression in 4-2B2, 4-5C8, and 4-5G9 clusters and a trend towards enrichment for *NKX6.1*, suggesting enrichment of INS$^+$PDX1$^+$NKX6.1$^+$ β cells over INS$^-$PDX1$^+$NKX6.1$^+$ pancreatic progenitors (Figure S2B). Expression of the endocrine marker *CHGA*, as well as other β cell markers, such as *UCN3* and *MAFA*, was increased in all sorted clusters, while expression of glucagon (*GCG*) was only statistically significantly increased in 4-2B2 and 4-5C8 clusters (Figure S2B), indicating that all three clones enrich for endocrine cells. In addition, the expression of the pluripotency markers *OCT4* and *SOX2* was significantly reduced in all sorted clusters when compared with pluripotent stem cells (Figure S2C).

We next evaluated the physiological properties of magnetically sorted eBCs to determine whether enrichment of β cells upon reaggregation is sufficient to promote an increase in their maturation, as observed in INS-GFP sorted eBCs (Nair et al., 2019b). We performed dynamic glucose-stimulated insulin secretion (GSIS) to test the response of eBCs to secretagogues such as glucose and KCl in a perifusion system. We first noted that the basal C-peptide secretion at a concentration of 2.8 mM glucose was increased in GFP, 4-2B2, and 4-5C8 eBCs when compared with unsorted clusters (Figure 3H). This increase in the amount of C-peptide secreted per 100 eBCs correlates with the higher proportions of C-peptide$^+$/NKX6.1$^+$ cells in reaggregated clusters (Figure 3G), confirming enrichment of β cells after sorting. Importantly, GFP sorted eBCs, as well as 4-2B2 and 4-5C8 eBCs, displayed a more pronounced first-phase response to high glucose compared with unsorted clusters, while the level of secretion was not significantly different for 4-5G9 eBCs (Figure 3H). These results thus indicated that magnetic sorting using the 4-2B2 and 4-5C8 mAbs recapitulates the increase in maturation seen in GFP sorted eBCs.

Sorting using the 4-2B2 and 4-5C8 clones also enriches for other endocrine cells

Although efforts to develop stem cell therapies for the treatment of diabetes have mostly focused on generating β cells, there are potential advantages in including other endocrine cells in the reaggregated clusters (Bru-Tari et al., 2020). Previous studies have shown the importance of other islet cell types in regulating insulin secretion (Capozzi et al., 2019; Rodriguez-Diaz et al., 2018; Wojtusciszyn et al., 2008), suggesting that generating islet-like reaggregates might be more beneficial than producing pure β cell clusters. To assess whether epitopes recognized by clones 4-2B2, 4-5C8, and 4-5G9 are expressed by other endocrine cells, we performed immunofluorescence staining of human pancreas sections using these newly generated mAbs. 4-2B2 staining was observed in both α and β cells within human islets, with the most intense labeling found in α cells, while 4-5C8 and 4-5G9 mAbs stained both α and β cells similarly (Figure 4A). These results thus suggest that all three clones mark adult α and β cells in human islets, with clone 4-2B2 staining α cells more strongly than β cells.

To verify whether clones 4-2B2, 4-5C8, and 4-5G9 can also enrich for hPSC-derived α and δ cells, we analyzed cells from the immature β-like stage using flow cytometry. We found that most glucagon-expressing cells were also strongly labeled with the 4-2B2 and 4-5C8 antibodies, while the staining with 4-5G9 was weaker, indicating that this clone might have a lower affinity for hPSC-derived α cells (Figure 4B). Next, we assessed whether our magnetic sorting strategy using the 4-2B2, 4-5C8, and 4-5G9 mAbs led to enrichment of α cells. We first quantified the percentage of glucagon-expressing cells in magnetically sorted eBCs and compared with unsorted and GFP sorted clusters as controls. We found that the proportion of glucagon-expressing cells was significantly higher in 4-2B2 and 4-5C8 eBCs, but not in 4-5G9 and GFP sorted eBCs (Figures 4C and 4D). Immunofluorescence staining of magnetically sorted eBCs confirmed the enrichment of both insulin- and glucagon-expressing cells in 4-2B2 and 4-5C8 eBCs (Figure 4E). Finally, flow cytometric analysis of magnetically sorted eBCs indicated that somatostatin-expressing cells were significantly enriched only in 4-5C8 eBCs (Figures 4F and 4G). These data thus demonstrate that some of the antibodies identified in our screening can be used to enrich for multiple types of stem cell-derived endocrine cells, broadening the potential benefit of these mAbs.

In vivo characterization of magnetically sorted eBCs

To test the growth potential of magnetically sorted eBCs *in vivo*, we transplanted clusters in immunodeficient mice and followed the development of grafts over time. Magnetically sorted eBCs were generated from a subline of INS-GFP that has been modified to constitutively express luciferase

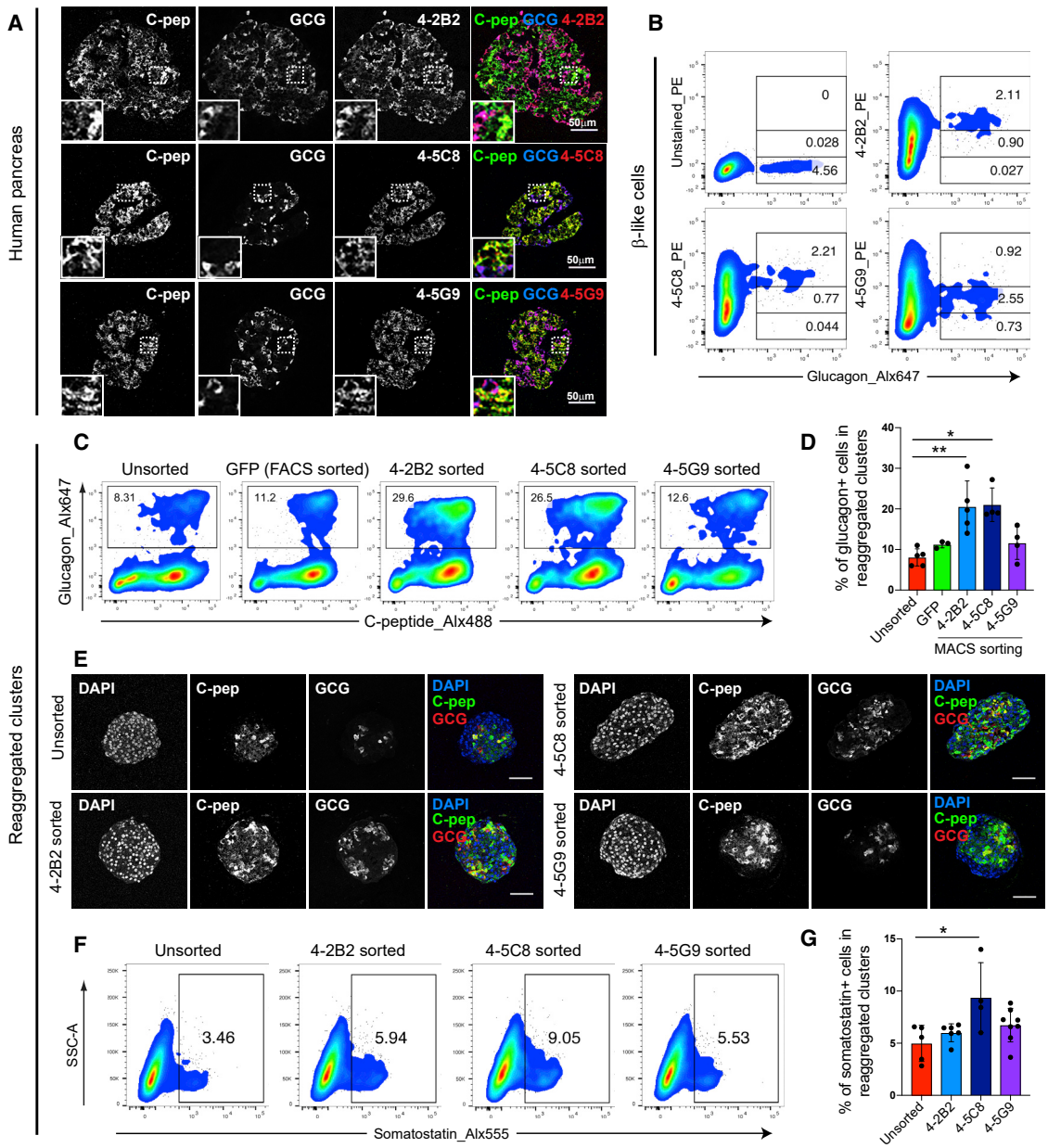

Figure 4. Sorting using the 4-2B2 and 4-5C8 clones also enriches for α cells

(A) Immunofluorescence analysis of human adult pancreas stained for C-peptide (C-pep, green), glucagon (GCG, blue), and the 4-2B2, 4-5C8, and 4-5G9 mAbs (red). Scale bars, 50 μm. (B) Flow cytometric analysis of glucagon and 4-2B2/4-5C8/4-5G9 co-expression at the β-like stage. Gates were drawn to quantify glucagon expression in cells strongly, weakly, or not labeled by the mAbs. (C and D) Representative FACS plots (C) and quantification (D) of glucagon$^+$ cells in unsorted, GFP FACS sorted, 4-2B2 MACS sorted, 4-5C8 MACS sorted, and 4-5G9 MACS sorted eBCs 1 week after enrichment. Data are represented as mean ± SD. Each point is an independent experiment. *$p < 0.05$ and **$p < 0.01$ determined by two-tailed unpaired t test. (E) Immunofluorescence images of unsorted, 4-2B2 sorted, 4-5C8 sorted, and 4-5G9 sorted clusters stained with DAPI (blue), C-peptide (C-pep, green), and glucagon (GCG, red). Scale bars, 50 μm. (F and G) Representative FACS plots (F) and quantification (G) of somatostatin$^+$ cells in unsorted, 4-2B2 sorted, 4-5C8 sorted, and 4-5G9 sorted eBCs 1 week after enrichment. Data are represented as mean ± SD. Each point is an independent experiment. *$p < 0.05$ determined by two-tailed unpaired t test.

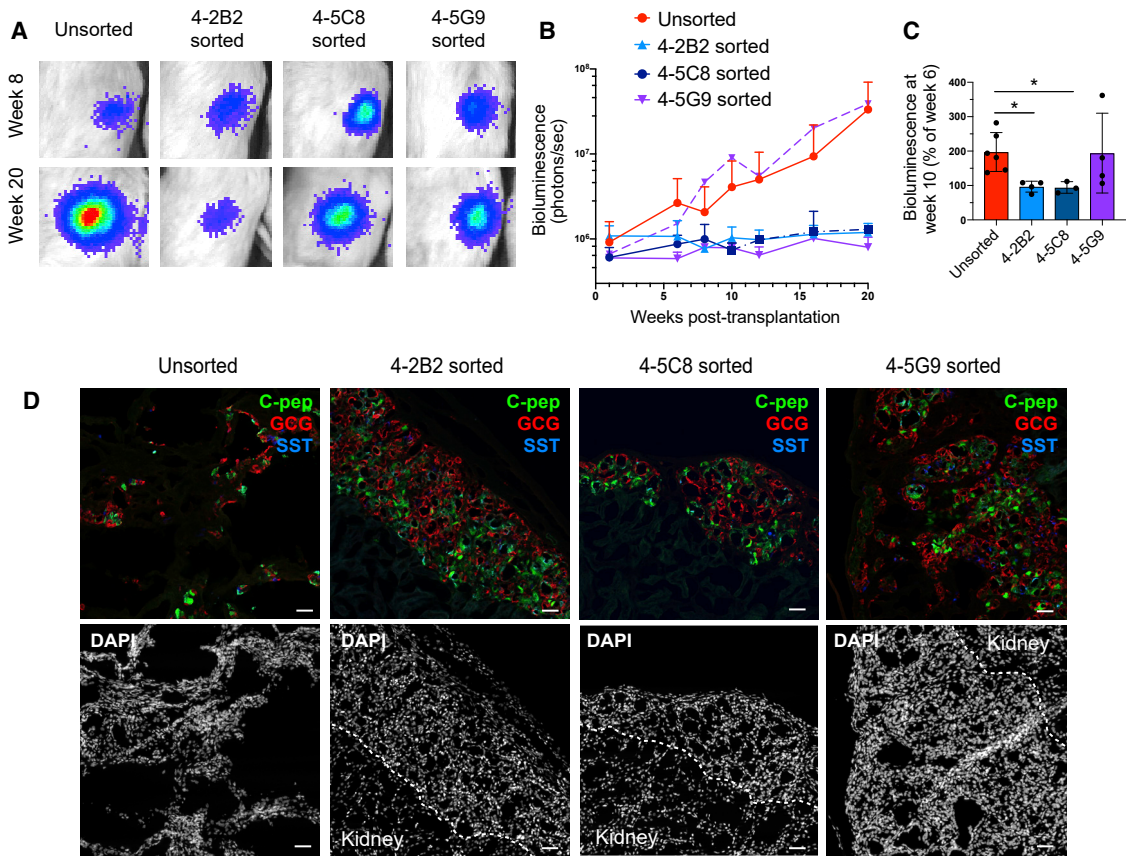

Figure 5. *In vivo* characterization of magnetically sorted eBCs

(A and B) NSG mice transplanted with unsorted, 4-2B2 sorted, 4-5C8 sorted, or 4-5G9 sorted clusters were monitored biweekly using non-invasive bioluminescence imaging to quantify changes in cell mass over time. Results for one representative mouse in each group are shown in (A), and the quantification for all mice is shown in (B). Dotted purple line represents data from one mouse transplanted with 4-5G9 sorted clusters that had higher signal than the rest of the group. n = 3–6 for all time points except weeks 12 (n = 2), 16 (n = 2), and 20 (n = 1) of the 4-5C8 group because of death of mice prior to the end of the experiment. This reduction in the number of animals is indicated by a change from a solid to a dotted line. (C) Quantification of bioluminescence levels at week 10. Results are shown as a percentage of week 6. *$p < 0.05$ as determined by two-tailed unpaired t test (n = 3–6). (D) Immunofluorescence images of unsorted, 4-2B2 sorted, 4-5C8 sorted, and 4-5G9 sorted grafts stained for C-peptide (C-pep, green), glucagon (GCG, red), and somatostatin (SST, blue). DAPI staining is shown in white in a separate panel. Dotted lines indicate the separation between graft and kidney. Scale bars, 50 μm. See also Figure S3.

in all cells to allow for non-invasive imaging of the cells (Faleo et al., 2017). This modification provided a linear relationship between bioluminescence emission and graft mass that could be tracked repeatedly and non-invasively for several weeks post-transplantation. We magnetically sorted immature β-like cells using the 4-2B2, 4-5C8, and 4-5G9 mAbs, reaggregated them to form eBCs, and transplanted them under the kidney capsule of non-diabetic NSG mice with unsorted cells as control. After injection of luciferin substrate into transplanted mice, bioluminescence was visible in an area consistent with the anatomical location of the engrafted cells (Figure 5A). The bioluminescence intensity was relatively consistent for 4-2B2 and 4-5C8 sorted clusters until week 20, the endpoint of our analysis, while unsorted cells showed an increase in signal suggestive of uncontrolled growth around week 10 post-transplantation (Figures 5A–5C). As for 4-5G9 sorted clusters, all grafts but one had consistent signal over time, suggesting that sorting with this antibody does improve engraftment outcome but might not remove proliferating cells as efficiently as the other two clones (Figure 5B). Isolation of kidneys confirmed the expansion of cells from unsorted clusters, whereas cells sorted with the 4-2B2 and 4-5C8 clones did not form enlarged structures and appeared similar in size to the initial transplant (Figure S3A). Notably, grafts of 4-5G9 sorted eBCs were more variable in size, with one animal showing a graft bigger than the original transplant (Figures 5B and S3A). Immunofluorescence analysis of harvested grafts confirmed that sorting with all three mAbs enriched for endocrine cells over unsorted

grafts (Figure 5D) and reduced Ki67$^+$vimentin$^+$ fibroblasts (Figure S3B), further validating the efficiency of these mAbs for excluding proliferative populations. These results thus indicate that magnetically sorted eBCs are less proliferative than unsorted clusters, making them safer for long-term transplantation.

Magnetic sorting of iPSC-derived islet cells

Given the interest in using induced pluripotent stem cells (iPSCs) to generate autologous stem cell derivatives for cell replacement therapies (Takahashi et al., 2007), we evaluated whether these newly generated mAbs can also function as positive selection markers for purification of iPSC-derived β cells. A commercially available iPSC line was differentiated up to the β-like stage using a slightly modified version of our differentiation protocol. To assess the ability of the mAbs to label iPSC-derived islet cells, we stained cells with the 4-2B2, 4-5C8, and 4-5G9 clones together with antibodies against C-peptide, NKX6.1, or glucagon. The percentage of positive cells in the population that was labeled with the 4-2B2, 4-5C8, or 4-5G9 mAbs was then quantified by flow cytometric analysis. As shown in Figures 6A and 6B, the 4-5G9$^+$ population contained significantly more C-peptide$^+$ and C-peptide$^+$/NKX6.1$^+$ than unstained, 4-2B2$^+$, and 4-5C8$^+$ populations, while glucagon$^+$ cells were enriched with all three clones compared with unstained. The 4-5G9 clone was thus selected for magnetic sorting and reaggregation of iPSC-derived β cells. Similar to what was observed with hESC-derived islet-like clusters, cells recovered after magnetic sorting with the 4-5G9 mAb reorganized into spheres of about 100–200 μm in pre-patterned micro-well plates (Figure 6C). Importantly, flow cytometric analysis of reaggregated clusters showed a significant enrichment in C-peptide$^+$ cells in 4-5G9 sorted clusters (57.1% ± 5.7%) over unsorted clusters (33.9% ± 9.4%), as well as in C-peptide$^+$/NKX6.1$^+$ cells (16.5% ± 7.4% in unsorted clusters versus 30.0% ± 7.2% in 4-5G9 clusters) (Figures 6D and 6E). Immunofluorescence analysis of iPSC-derived islet-like clusters confirmed the presence of insulin$^+$/PDX1$^+$/NKX6.1$^+$ cells in the 4-5G9 eBCs (Figure 6F). Taken together, these data demonstrate that the scalable magnetic sorting method developed with the INS-GFP hESC line can be adapted to generate enriched islet-like clusters from iPSCs.

DISCUSSION

The regenerative biology field has seen remarkable progress with regard to *in vitro* differentiation of hPSCs into functional β cells. However, there is still a need for scalable purification methods for isolating such a population of cells for transplantation. Here, we developed a purification protocol that is scalable and does not require the use of a fluorescent reporter by generating and screening more than a thousand mAbs against cell surface markers expressed on stem cell-derived pancreatic cells. This approach identified several promising candidate antibodies, including three clones that were further validated for their ability to enrich for islet cells in differentiated cultures using a magnetic sorting strategy. Importantly, this work confirmed that enriching for endocrine cells using this scalable method improves the ability of hPSC-derived islet-like clusters to respond to glucose while reducing their proliferative potential *in vivo*.

Previous studies have reported strategies to enrich for anterior definitive endoderm (Mahaddalkar et al., 2020) or pancreatic progenitors (Ameri et al., 2017; Cogger et al., 2017; Kelly et al., 2011). However, the resulting clusters had lower percentages of C-peptide$^+$ cells than GFP sorted eBCs (<50% compared with approximately 80% in GFP sorted eBCs). Recent studies also described methods to sort β cells from hPSC differentiations using the cell surface marker CD49a or the dye N-(6-methoxy-8-quinolyl)-p-toluenesulfonamide (TSQ) (Davis et al., 2019; Veres et al., 2019). These protocols led to the formation of clusters highly enriched for β cells, but <10% of insulin$^+$ cells were recovered following these procedures, likely impeding their use for applications that require large numbers of cells. In contrast, magnetic sorting using the 4-2B2, 4-5C8, and 4-5G9 clones produced clusters with >70% insulin-expressing cells with a percentage of recovery of C-peptide$^+$ cells ranging from 30% to 50%. The use of these new mAbs thus has the potential to increase the scalability of this purification step by improving both the purity and the yield.

Although the enrichment for C-peptide$^+$ cells following magnetic sorting was significant for all three clones, only 4-2B2 and 4-5C8 sorted clusters showed improved function over unsorted clusters. One possible explanation for this observation is that the proportion of C-peptide$^+$/NKX6.1$^+$ cells in reaggregated clusters needs to be increased above a certain threshold to observe the improvement in β cell function. The percentage of C-peptide$^+$/NKX6.1$^+$ cells in 4-2B2 and 4-5C8 sorted clusters was indeed more similar to the one obtained with FACS using the INS-GFP reporter line than in the 4-5G9 sorted clusters. Alternatively, it is possible that purification using GFP or the 4-2B2/4-5C8 clones eliminates cell types that affect function in unsorted clusters, while sorting with the 4-5G9 clone does not. In addition, sorting with the 4-2B2 and 4-5C8 antibodies led to increased recovery of glucagon-expressing cells compared with unsorted and 4-5G9 sorted clusters. The final composition of reaggregated clusters formed after sorting with the 4-2B2 and 4-5C8 clones was closer to the composition of human islets, which contain on average

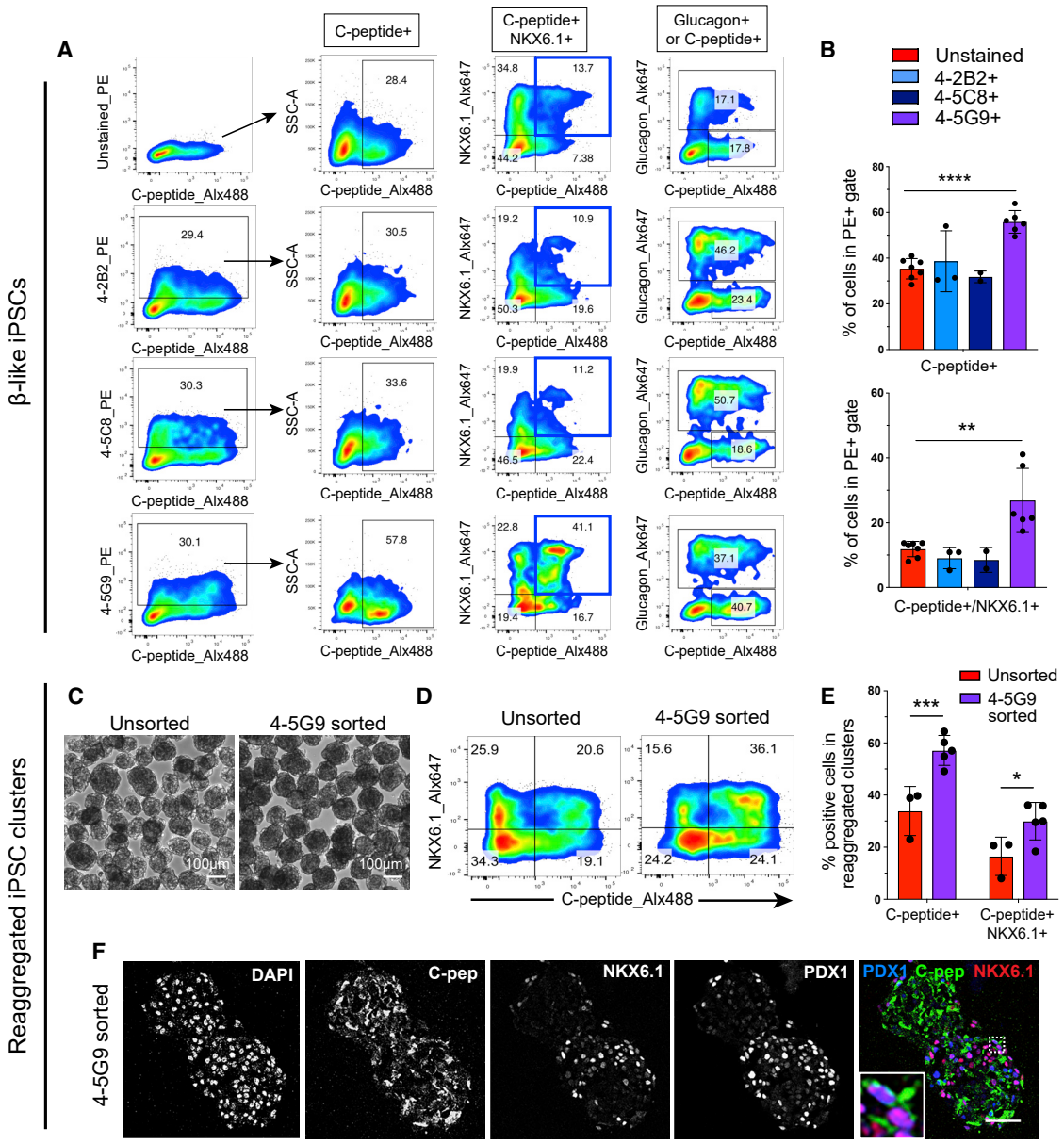

Figure 6. Magnetic sorting of iPSC-derived islet cells

(A) Representative FACS plots (A) and quantification (B) of C-peptide, NKX6.1, and glucagon expression in iPSC-derived β-like cells labeled with the 4-2B2, 4-5C8, or 4-5G9 mAbs. The percentage of positive cells is quantified in non-gated samples for the unstained control or after pre-gating to include the cells with the strongest labeling for each mAb (top 30%). Data are represented as mean ± SD. $^{**}p < 0.01$ and $^{****}p < 0.0001$ determined by two-tailed unpaired t test. (C) Bright-field images of unsorted and 4-5G9 sorted clusters 1 week after magnetic enrichment. Scale bars, 100 μm. (D and E) Representative FACS plots (D) and quantification (E) of C-peptide$^+$ and NKX6.1$^+$ cells in iPSC-derived unsorted and 4-5G9 MACS sorted clusters 1 week after enrichment. Data are represented as mean ± SD. Each point is an independent experiment. $^{*}p < 0.05$ and $^{***}p < 0.001$ determined by two-tailed unpaired t test. (F) Immunofluorescence images of unsorted and 4-5G9 sorted iPSC-derived clusters stained with DAPI, C-peptide (C-pep, green), NKX6.1 (red), and PDX1 (blue). Scale bar, 50 μm.

38% α cells (Cabrera et al., 2006). Whereas variations in α cell numbers have been shown to affect β cell function and glycemic set point (Rodriguez-Diaz et al., 2018; Wojtusciszyn et al., 2008), additional studies are needed to assess the impact of increased numbers of glucagon- and somatostatin-expressing cells in hPSC-derived islet-like clusters. It will indeed be interesting to evaluate whether enriching for α and δ cells along with β cells recapitulates

the effect of proglucagon and somatostatin peptides secretion or cell-cell contacts on regulation of insulin secretion described for primary islets (Capozzi et al., 2019; Huising et al., 2018; Wojtusciszyn et al., 2008).

Finally, although all three mAbs stained both hESC- and iPSC-derived islet cells, there were differences in their ability to enrich for different cell types when sorting at the β-like stage. Clones 4-2B2 and 4-5C8 were indeed more efficient at enriching for C-peptide$^+$/NKX6.1$^+$ from hESCs, while clone 4-5G9 performed better with iPSC-derived β-like cells. It is therefore likely that the level and/or timing of expression of the epitope recognized by these mAbs varies between cell lines. A thorough assessment of the dynamics of expression for each mAb might be required when optimizing the sorting method for islet cells derived from different hPSC lines.

In summary, we optimized scalable purification conditions that allow for the recovery of a greater fraction of insulin- and glucagon-expressing cells from hPSC pancreatic differentiations while increasing β cell function and graft safety upon prolonged engraftment. Magnetic sorting using these new antibodies should therefore facilitate the production of large amounts of functional islet-like clusters suitable for diverse *in vitro* and *in vivo* applications, potentially accelerating the translation of stem cell replacement therapies for patients with diabetes.

EXPERIMENTAL PROCEDURES

Culture of pluripotent cells

Experiments were performed using the NIH-approved hESC line MEL-1 (NIH registration number: 0139), in which a GFP was knocked into one allele of the endogenous insulin locus (INS$^{GFP/W}$ hESCs) (Micallef et al., 2011). The human iPSC line was purchased from Thermo Fisher Scientific (#A18945). Both hPSC lines were cultured on irradiated mouse embryonic fibroblasts (MEFs) (Thermo Fisher) in hESC maintenance media composed of DMEM/F12, 20% (v/v) KnockOut serum replacement (Thermo Fisher Scientific), nonessential amino acids (Thermo Fisher Scientific), GlutaMAX (Thermo Fisher Scientific), and 2-mercaptoethanol (Millipore). The maintenance media was supplemented with 4 ng/mL recombinant human fibroblast growth factor 2 (FGF-2; R&D Systems). For iPSC culture, the maintenance media were also supplemented with 10 ng/mL activin A (R&D Systems). Confluent hPSCs were dissociated into single-cell suspension by incubation with TrypLE Select (Gibco) and passaged every 3–4 days. G-banded karyotyping performed by Cell Line Genetics confirmed normal karyotype of INS$^{GFP/W}$ hESCs. Cells have been confirmed to be mycoplasma-free using the MycoProbe Mycoplasma Detection Kit (R&D Systems) or the Venor GeM Mycoplasma Detection Kit (Sigma).

Differentiation into pancreatic cells

To initiate differentiation, we dissociated confluent cultures into single-cell suspensions using TrypLE Select, counted them, and seeded them in six-well suspension plates at a density of 5.5 × 10^6 cells per 5.5 mL of hESC maintenance media supplemented with 10 ng/mL activin A (R&D Systems) and 10 ng/mL heregulinB (PeproTech). The plates were incubated at 37°C and 5% CO_2 on an orbital shaker set at 100 rpm to induce 3D sphere formation. After 24 h, the spheres were differentiated as previously described (Nair et al., 2019a, 2019b). Spheres were collected in 50-mL tubes, allowed to settle by gravity, washed once with PBS or RPMI (Gibco), and re-suspended in d1 differentiation media. The resuspended spheres were distributed into fresh six-well suspension plates for a final volume of 5.5 mL of d1 media per well. Until d3, spheres were fed daily by removing media and replenishing with 5.5 mL of fresh media. From d4 to d20, media was removed daily, and 5 mL of fresh media was added. Media compositions for differentiation of INS$^{GFP/W}$ hESCs are as follows: d1, RPMI (Gibco) containing 0.2% FBS, 1:5,000 ITS (Gibco), 100 ng/mL activin A, and 50 ng/mL WNT3a (R&D Systems); d2, RPMI containing 0.2% FBS, 1:2,000 ITS, and 100 ng/mL activin A; d3, RPMI containing 0.2% FBS, 1:1,000 ITS, 2.5 μM TGFbi IV (Calbiochem), and 25 ng/mL keratinocyte growth factor (KGF; R&D Systems); d4–5, RPMI containing 0.4% FBS, 1:1,000 ITS, and 25 ng/mL KGF; d6–7, DMEM (Gibco) with 25 mM glucose containing 1:100 B27 (Gibco) and 3 nM TTNPB (Sigma); d8, DMEM with 25 mM glucose containing 1:100 B27, 3 nM TTNPB, and 50 ng/mL epidermal growth factor (EGF; R&D Systems); d9–11, DMEM with 25 mM glucose containing 1:100 B27, 50 ng/mL EGF, and 50 ng/mL KGF; d12+, DMEM with 25 mM glucose containing 1:100 B27, 1:100 GlutaMAX (Gibco), 1:100 NEAA (Gibco), 10 μm ALKi II (Axxora), 500 nM LDN-193189 (Stemgent), 1 μm Xxi (Millipore), 1 μM T3 (Sigma-Aldrich), 0.5 mM vitamin C, 1 mM *N*-acetylcysteine (Sigma-Aldrich),10 μM zinc sulfate (Sigma-Aldrich), and 10 μg/mL heparin sulfate. For iPSC differentiation, media compositions were similar except that 1 μM of the PI3K inhibitor LY294002 (Cayman Chemicals) was added to d1 media, and the d9–11 stage was extended to d14.

For immunization experiments, MEL1 INS$^{GFP/W}$ hESCs differentiated up to d19–20 were sorted into GFP$^+$ and GFP$^-$ fractions according to the method described in the *FACS sorting* section (supplemental experimental procedures). The GFP$^+$ fraction was reaggregated in six-well suspension plates at a concentration of 1 million cells/mL in d12+ media, while the GFP$^-$ fraction was seeded in d12+ media without ALKi II and T3 to reduce further specification of endocrine cells. Both media were supplemented with 10 μM of the ROCK inhibitor Y-27632 (Tocris) and penicillin-streptomycin (Corning). The plates were incubated at 37°C and 5% CO_2 on an orbital shaker set at 100 rpm to induce 3D sphere formation. Cells were injected into mice 3 days later.

Immunization and antibody generation

For generation of antibodies against specific epitopes, a subtractive immunization strategy was employed (Williams et al., 1992), and the immunizations were performed under a protocol approved by the Oregon Health and Science University (OHSU) Institutional Animal Care and Use Committee. Two mice were inoculated intraperitoneally (i.p.) with either GFP$^+$ or GFP$^-$ sorted β-like clusters followed by cyclophosphamide injection 24–48 h later to eliminate B lymphocytes reacting against these antigens. Mice were then inoculated with the opposite clusters (the mouse that initially

received GFP^+ cells was injected with GFP^- cells and vice versa) after 4 weeks and one more time 18–21 weeks after the initial injection. Animals were euthanized 4 days after the final immunization and their spleen harvested. Splenocytes were fused with SP2/0-Ag14 myeloma cells using polyethylene glycol and selected by growth in methylcellulose containing hypoxanthine-aminopterin-thymidine (HAT) medium. A total of 1,248 isolated clones were transferred to liquid medium in 96-well plates. Supernatants were then screened by flow cytometry as described in the following section, *Antibody screening*.

Antibody screening

Mel1 $INS^{GFP/W}$ hESCs were differentiated up to d19–23 according to the protocol detailed earlier in the section *Differentiation into pancreatic cells*. The spheres were dissociated for 8–10 min using Accumax (Thermo Fisher Scientific) prior to quenching with FACS buffer (2% FBS and 2 mM EDTA in PBS without calcium and magnesium). Approximately 30,000–50,000 cells were plated in a 96-well V-bottom plate. The cells were stained with 35 μL undiluted hybridoma supernatant for 30 min at 4°C–8°C, washed twice with FACS buffer, followed by staining with an anti-mouse secondary antibody conjugated to R-phycoerythrin (PE) for 25 min at 4°C–8°C. At the end of the incubation, cells were washed twice with FACS buffer prior to suspension in FACS buffer with DAPI. Flow cytometric analysis was performed using a High-Throughput Sampler (HTS) device connected to a BD Fortessa X20 cytometer (BD Biosciences).

Magnetic sorting

Mel1 $INS^{GFP/W}$ hESCs or iPSCs differentiated up to the β-like stage were collected from suspension plates (d19–21 for $INS^{GFP/W}$ hESCs and d21–23 for iPSCs) and dissociated into single cells with Accumax. The cells were quenched with sorting buffer (0.5% BSA, 2 mM EDTA, and 10 μM ROCK inhibitor in PBS without calcium and magnesium), filtered through a 0.35-μm mesh, centrifuged, counted, and resuspended in sorting buffer at a density of 50 million cells/mL. An aliquot of cells was collected prior to staining and reaggregated as unsorted control. Cells were then stained with 4-2B2, 4-5C8, or 4-5G9 hybridoma supernatants for 30 min at 4C–8C with constant agitation. After washing with sorting buffer, cells were resuspended in 80 μL of sorting buffer per 10^7 cells, and anti-mouse IgM MicroBeads (catalog #130-047-301; Miltenyi Biotec) were added at a concentration of 15 μL per 10^7 cells. The cells were incubated with microbeads for 20 min at 4C–8C with constant agitation. Cells were washed and resuspended in 500 μL of sorting buffer (up to 10^8 cells) prior to magnetic separation on LS columns and suitable MACS Separator (Miltenyi Biotec). Columns were rinsed with an appropriate amount of MACS buffer prior to loading of the cell suspension. After washing three times with 3 mL of MACS buffer, the column was removed from the separator and cells were eluted using 5 mL of sorting buffer. After taking an aliquot for flow cytometric analysis to verify enrichment, the rest of the cells were counted and seeded into AggreWell plates using the protocol outlined in the *FACS sorting* section (supplemental experimental procedures). Alternatively, sorted cells were reaggregated directly in six-well suspension plates by seeding them at a concentration of 2 million cells in 3 mL of reaggregation media per well. Two to three days later, clusters reaggregated in AggreWell plates were transferred to six-well suspension plates and placed on an orbital shaker set at 100 rpm. Clusters were further cultured for up to 10 days. Media were changed every third day following reaggregation.

Dynamic perifusion assay for GSIS

Dynamic GSIS was performed using a perifusion system (Biorep Technologies) as previously described (Nair et al., 2019b). For each sample, 100 sorted clusters were handpicked and placed on filters in plastic chambers that were maintained under temperature- and CO_2-controlled conditions. After an initial 1- to 2-h preincubation period in 2.8 mM glucose in Krebs-Ringer Bicarbonate (KRB) buffer, chambers were sequentially perifused at a flow rate of 100 μL/min with 2.8 mM glucose for 20 min, 20 mM glucose for 30 min, 2.8 mM glucose for 20 min, and 2.8 mM glucose/30 mM KCL for 15 min. Flow-through was collected over the course of the experiment, and insulin concentrations in the supernatant were determined using an ultrasensitive insulin ELISA kit (STELLUX Chemi Human C-peptide ELISA; Alpco). The insulin secretion levels were normalized by total cell number (pg per mL per 100 clusters).

Mouse transplantation studies

NSG mice were obtained from Jackson Laboratories and bred in University of California San Francisco (UCSF) facilities. Both male and female mice between 6 and 16 weeks of age were used in this study. Sorted clusters were transplanted under the kidney capsule of mice (~2.5–3 × 10^6 cells per mouse) according to protocols approved by the UCSF Institutional Animal Care and Use Committee. Transplanted mice were injected i.p. with 15 mg/mL D-luciferin solution (Goldbio Biotechnology) before imaging on a Xenogen IVIS 200 imaging system (Perkin Elmer). Signals were acquired and analyzed using the Living Image analysis software (Xenogen). Same-sized regions of interests were manually drawn for the analysis of all data points within the same experiment to ensure consistency in signal quantification. Kidneys bearing grafts were removed at indicated time points, embedded in optimal cutting temperature (OCT) for cryopreservation, and sectioned for immunofluorescence as described above.

Sampling and statistical analysis

Each experiment was performed unblinded on different biological groups with multiple biological replicates. No statistical analysis was done *a priori* to determine the sample sizes. Statistical tests performed for specific datasets are described in the corresponding figure legends. All statistical tests were performed in GraphPad Prism Software. Experiments in the study were repeated independently at least three times except where indicated.

Data and code availability

This study did not generate any code.

SUPPLEMENTAL INFORMATION

Supplemental information can be found online at https://doi.org/10.1016/j.stemcr.2022.02.001.

AUTHOR CONTRIBUTIONS

Conceptualization, A.V.P., J.S.L., P.R.S., and M.H.; investigation, A.V.P, S.A., G.G.N., M.-L.L., J.C., J.S.L., and Y.Z.; writing – original draft, A.V.P. and S.A.; writing – review & editing, A.V.P., S.A., J.S.L., P.R.S., and M.H.

CONFLICT OF INTERESTS

M.H. is on the Scientific Advisory Board (SAB) of Encellin Inc. and Thymmune Therapeutics Inc.; holds stocks in Encellin Inc., Thymmune Therapeutics Inc., and Viacyte Inc.; and has received research support from Eli Lilly. He is the co-founder and SAB member of Minutia Inc. and EndoCrine and holds stocks and options in both companies. A.V.P. is on the SAB of Thymmune Therapeutics and holds stock options in the company.

ACKNOWLEDGMENTS

We would like to thank members of the Hebrok laboratory for helpful discussions. Work in M.H.'s laboratory was supported by a grant from the NSF (1743407). Imaging and flow cytometry experiments were supported by resources from the UCSF Diabetes and Endocrinology Research Center (DRC) and UCSF Flow Cytometry Core (NIH Diabetes Research Center grant P30 DK063720). G.G.N. was supported by a Kraft Family Fellowship and a JDRF postdoctoral fellowship (1-PNF-2016-320-S-B), S.A. by a Larry L. Hillblom Foundation fellowship, and J.S.L. by a Kraft Family Fellowship and a T32 training grant (T32CA177555-02).

Received: February 23, 2021
Revised: January 31, 2022
Accepted: February 1, 2022
Published: March 3, 2022

REFERENCES

Ameri, J., Borup, R., Prawiro, C., Ramond, C., Schachter, K.A., Scharfmann, R., and Semb, H. (2017). Efficient generation of glucose-responsive beta cells from isolated GP2+ human pancreatic progenitors. Cell Rep. *19*, 36–49. https://doi.org/10.1016/j.celrep.2017.03.032.

Bru-Tari, E., Oropeza, D., and Herrera, P.L. (2020). Cell heterogeneity and paracrine interactions in human islet function: a perspective focused in β-cell regeneration strategies. Front Endocrinol. (Lausanne) *11*, 619150. https://doi.org/10.3389/fendo.2020.619150.

Cabrera, O., Berman, D.M., Kenyon, N.S., Ricordi, C., Berggren, P.-O., and Caicedo, A. (2006). The unique cytoarchitecture of human pancreatic islets has implications for islet cell function. Proc. Natl. Acad. Sci. U.S.A. *103*, 2334–2339. https://doi.org/10.1073/pnas.0510790103.

Capozzi, M.E., Svendsen, B., Encisco, S.E., Lewandowski, S.L., Martin, M.D., Lin, H., Jaffe, J.L., Coch, R.W., Haldeman, J.M., MacDonald, P.E., et al. (2019). β Cell tone is defined by proglucagon peptides through cAMP signaling. JCI Insight *4*. https://doi.org/10.1172/jci.insight.126742.

Cogger, K.F., Sinha, A., Sarangi, F., McGaugh, E.C., Saunders, D., Dorrell, C., Mejia-Guerrero, S., Aghazadeh, Y., Rourke, J.L., Screaton, R.A., et al. (2017). Glycoprotein 2 is a specific cell surface marker of human pancreatic progenitors. Nat. Commun. *8*, 331. https://doi.org/10.1038/s41467-017-00561-0.

Davis, J.C., Helman, A., Rivera-Feliciano, J., Langston, C.M., Engquist, E.N., and Melton, D.A. (2019). Live cell monitoring and enrichment of stem cell-derived β cells using intracellular zinc content as a population marker. Curr. Protoc. Stem Cell Biol. *51*, e99. https://doi.org/10.1002/cpsc.99.

Dorrell, C., Abraham, S.L., Lanxon-Cookson, K.M., Canaday, P.S., Streeter, P.R., and Grompe, M. (2008). Isolation of major pancreatic cell types and long-term culture-initiating cells using novel human surface markers. Stem Cell Res. *1*, 183–194. https://doi.org/10.1016/j.scr.2008.04.001.

Dorrell, C., Schug, J., Canaday, P.S., Russ, H.A., Tarlow, B.D., Grompe, M.T., Horton, T., Hebrok, M., Streeter, P.R., Kaestner, K.H., and Grompe, M. (2016). Human islets contain four distinct subtypes of β cells. Nat. Commun. *7*, 11756. https://doi.org/10.1038/ncomms11756.

Faleo, G., Russ, H.A., Wisel, S., Parent, A.V., Nguyen, V., Nair, G.G., Freise, J.E., Villanueva, K.E., Szot, G.L., Hebrok, M., and Tang, Q. (2017). Mitigating ischemic injury of stem cell-derived insulin-producing cells after transplant. Stem Cell Rep. *9*, 807–819. https://doi.org/10.1016/j.stemcr.2017.07.012.

Huising, M.O., van der Meulen, T., Huang, J.L., Pourhosseinzadeh, M.S., and Noguchi, G.M. (2018). The difference δ-cells make in glucose control. Physiology (Bethesda) *33*, 403–411. https://doi.org/10.1152/physiol.00029.2018.

Kelly, O.G., Chan, M.Y., Martinson, L.A., Kadoya, K., Ostertag, T.M., Ross, K.G., Richardson, M., Carpenter, M.K., D'Amour, K.A., Kroon, E., et al. (2011). Cell-surface markers for the isolation of pancreatic cell types derived from human embryonic stem cells. Nat. Biotechnol. *29*, 750–756. https://doi.org/10.1038/nbt.1931.

Mahaddalkar, P.U., Scheibner, K., Pfluger, S., Ansarullah, Sterr, M., Beckenbauer, J., Irmler, M., Beckers, J., Knöbel, S., and Lickert, H. (2020). Generation of pancreatic β cells from CD177+ anterior definitive endoderm. Nat. Biotechnol. *38*, 1061–1072. https://doi.org/10.1038/s41587-020-0492-5.

Micallef, S.J., Li, X., Schiesser, J.V., Hirst, C.E., Yu, Q.C., Lim, S.M., Nostro, M.C., Elliott, D.A., Sarangi, F., Harrison, L.C., et al. (2011). INS GFP/w human embryonic stem cells facilitate isolation of in vitro derived insulin-producing cells. Diabetologia *55*, 694–706. https://doi.org/10.1007/s00125-011-2379-y.

Nair, G., Russ, H., and Hebrok, M. (2019a). Rapid generation of functional mature pancreatic islet-beta cells from human pluripotent stem cells. Protoc. Exchange https://doi.org/10.1038/protex.2018.140.

Nair, G.G., Liu, J.S., Russ, H.A., Tran, S., Saxton, M.S., Chen, R., Juang, C., Li, M.-L., Nguyen, V.Q., Giacometti, S., et al. (2019b). Recapitulating endocrine cell clustering in culture promotes maturation of human stem-cell-derived β cells. Nat. Cell Biol. *21*, 263–274. https://doi.org/10.1038/s41556-018-0271-4.

Nair, G.G., Tzanakakis, E.S., and Hebrok, M. (2020). Emerging routes to the generation of functional β-cells for diabetes mellitus

cell therapy. Nat. Rev. Endocrinol. *16*, 506–518. https://doi.org/10.1038/s41574-020-0375-3.

Pagliuca, F.W., Millman, J.R., Gürtler, M., Segel, M., Van Dervort, A., Ryu, J.H., Peterson, Q.P., Greiner, D., and Melton, D.A. (2014). Generation of functional human pancreatic b cells in vitro. CELL *159*, 428–439. https://doi.org/10.1016/j.cell.2014.09.040.

Pisania, A., Weir, G.C., O'Neil, J.J., Omer, A., Tchipashvili, V., Lei, J., Colton, C.K., and Bonner-Weir, S. (2010). Quantitative analysis of cell composition and purity of human pancreatic islet preparations. Lab. Invest. *90*, 1661–1675. https://doi.org/10.1038/labinvest.2010.124.

Rezania, A., Bruin, J.E., Arora, P., Rubin, A., Batushansky, I., Asadi, A., O'Dwyer, S., Quiskamp, N., Mojibian, M., Albrecht, T., et al. (2014). Reversal of diabetes with insulin-producing cells derived in vitro from human pluripotent stem cells. Nat. Biotechnol. https://doi.org/10.1038/nbt.3033.

Rodriguez-Diaz, R., Molano, R.D., Weitz, J.R., Abdulreda, M.H., Berman, D.M., Leibiger, B., Leibiger, I.B., Kenyon, N.S., Ricordi, C., Pileggi, A., et al. (2018). Paracrine interactions within the pancreatic islet determine the glycemic set point. Cell Metab. *27*, 549–558.e4. https://doi.org/10.1016/j.cmet.2018.01.015.

Russ, H.A., Parent, A.V., Ringler, J.J., Hennings, T.G., Nair, G.G., Shveygert, M., Guo, T., Puri, S., Haataja, L., Cirulli, V., et al. (2015). Controlled induction of human pancreatic progenitors produces functional beta-like cells in vitro. EMBO J. https://doi.org/10.15252/embj.201591058.

Russell, R., Carnese, P.P., Hennings, T.G., Walker, E.M., Russ, H.A., Liu, J.S., Giacometti, S., Stein, R., and Hebrok, M. (2020). Loss of the transcription factor MAFB limits β-cell derivation from human PSCs. Nat. Commun. *11*, 2742. https://doi.org/10.1038/s41467-020-16550-9.

Sneddon, J.B., Tang, Q., Stock, P., Bluestone, J.A., Roy, S., Desai, T., and Hebrok, M. (2018). Stem cell therapies for treating diabetes: progress and remaining challenges. Cell Stem Cell *22*, 810–823. https://doi.org/10.1016/j.stem.2018.05.016.

Takahashi, K., Tanabe, K., Ohnuki, M., Narita, M., Ichisaka, T., Tomoda, K., and Yamanaka, S. (2007). Induction of pluripotent stem cells from adult human fibroblasts by defined factors. CELL *131*, 861–872. https://doi.org/10.1016/j.cell.2007.11.019.

Velazco-Cruz, L., Song, J., Maxwell, K.G., Goedegebuure, M.M., Augsornworawat, P., Hogrebe, N.J., and Millman, J.R. (2019). Acquisition of dynamic function in human stem cell-derived β cells. Stem Cell Rep. *12*, 351–365. https://doi.org/10.1016/j.stemcr.2018.12.012.

Veres, A., Faust, A.L., Bushnell, H.L., Engquist, E.N., Kenty, J.H.-R., Harb, G., Poh, Y.-C., Sintov, E., Gürtler, M., Pagliuca, F.W., et al. (2019). Charting cellular identity during human in vitro β-cell differentiation. Nature *569*, 368–373. https://doi.org/10.1038/s41586-019-1168-5.

Williams, C.V., Stechmann, C.L., and McLoon, S.C. (1992). Subtractive immunization techniques for the production of monoclonal antibodies to rare antigens. Biotechniques *12*, 842–847.

Wojtusciszyn, A., Armanet, M., Morel, P., Berney, T., and Bosco, D. (2008). Insulin secretion from human beta cells is heterogeneous and dependent on cell-to-cell contacts. Diabetologia *51*, 1843–1852. https://doi.org/10.1007/s00125-008-1103-z.